

*Letter to the Editor***Mid-IR colors and star formation in Virgo and Coma galaxies\***

**A. Boselli<sup>1</sup>, J. Lequeux<sup>2</sup>, A. Contursi<sup>2</sup>, G. Gavazzi<sup>3</sup>, O. Boulade<sup>4</sup>, F. Boulanger<sup>5</sup>, D. Cesarsky<sup>5</sup>, C. Dupraz<sup>6</sup>, S. Madden<sup>4</sup>, M. Sauvage<sup>4</sup>, F. Viallefond<sup>2</sup>, and L. Vigroux<sup>4</sup>**

<sup>1</sup> Laboratoire d'Astronomie Spatiale, Traverse du Siphon, BP 8, F-13376 Marseille CEDEX 12, France

<sup>2</sup> Observatoire de Paris, 61 Av. de l'Observatoire, F-75014 Paris, France

<sup>3</sup> Università degli studi di Milano, Dipartimento di Fisica, Via Celoria 16, I-20121 Milano, Italy

<sup>4</sup> Service d'Astrophysique, Centre d'Etudes de Saclay, F-91191 Gif sur Yvette, France

<sup>5</sup> Institut d'Astrophysique Spatiale, Bat. 121, Université Paris-Sud, F-91405 Orsay, France

<sup>6</sup> Radioastronomie, Ecole Normale Supérieure, 24 Rue Lhomond, F-75231 Paris CEDEX 05, France

Received 17 January 1997 / Accepted 23 May 1997

**Abstract.** We present observations of the global emission of a sample of spiral and irregular galaxies in the Virgo cluster and the Coma supercluster. These observations have been made with the camera ISOCAM on board the Infrared Space Observatory, through two broad filters centered respectively at 6.75 and 15.0  $\mu\text{m}$ . The corresponding fluxes are corrected for the stellar contribution in order to obtain the pure interstellar contribution; the stellar contribution is estimated from the near-infrared fluxes using as template some S0 and elliptical galaxies observed by chance in the ISO fields. The fluxes at 6.75 and 15.0  $\mu\text{m}$  are then normalized to the stellar mass of the galaxy, and compared to the normalized far-UV fluxes at 2000 Å which are good indicators of the star-formation rate (SFR). We find that, while the mid-IR fluxes are proportional to the SFR when it is not too large, the galaxies with a high SFR have relatively less emission at 6.75 and 15  $\mu\text{m}$ . It appears that the carriers of the Unidentified Infrared Bands which are responsible for almost all the emission at 6.75  $\mu\text{m}$  and for a part of the emission at 15  $\mu\text{m}$  have different properties in these galaxies or are partly destroyed by the UV field. At 15  $\mu\text{m}$ , there is a contribution of very small, three-dimensional grains in galaxies with a high SFR.

**Key words:** Galaxies: general– Galaxies: ISM– Galaxies: spiral– Infrared: galaxies– Infrared: ISM: continuum

*Send offprint requests to:* A. Boselli boselli@astrsp-mrs.fr

\* Based on observations with ISO, an ESA project with instruments funded by ESA member states (especially the PI countries: France, Germany, the Netherlands and the United Kingdom) and with participation of ISAS and NASA

**1. Introduction**

The emission of the interstellar medium in the mid-IR is due to the Unidentified Infrared Emission Bands (UIBs) and in some conditions to the emission of very small, three-dimensional grains (Désert et al. 1990).

In order to understand better this emission, we have constructed a coherent program of observations with the Infrared Space Observatory (ISO), which includes a variety of Galactic objects which can be studied in details, objects in the Magellanic Clouds, larger regions in more distant galaxies like M 31, M 33, M 101, M 51 etc., then whole galaxies at larger distances in the Virgo cluster and the Coma supercluster. This paper is concerned with observations of a sample of the latter galaxies with ISOCAM through the two broad filters LW2 and LW3, which are centered respectively at 6.75 and 15  $\mu\text{m}$ .

Section 2 describes the sample and the observations; Section 3 discusses the normalized mid-IR fluxes and colors in relation to the star-formation rate (SFR). Section 4 contains the conclusions.

**2. Sample of galaxies and observations**

The selection of the Virgo galaxies observed by ISO is described extensively by Boselli et al. (1997). Shortly, this is a complete sample of late-type and S0/a galaxies brighter than  $B_T = 18$  mag. ( $M_B \leq -13$ ), selected from Binggeli et al. (1985). 99 galaxies have been observed with ISOCAM with a detection rate of 70% in the LW2 filter and 55% in the LW3 filter. A few other galaxies, including ellipticals, were included serendipitously in the observed fields. For the Coma supercluster, the sample is not complete in any sense, and comprises 18 late-type galaxies selected as exhibiting signs of interaction with the intergalactic medium and/or a strong star-formation activity. This sample

has been added to increase the relatively limited statistics, but the conclusions we derive could have been based on the Virgo sample alone. All the Coma supercluster galaxies have been detected in the LW2 and LW3 filters. We will use data at other wavelengths (far-IR, near-IR, far-UV) for comparison.

All the galaxies have been observed in the same way with ISOCAM. The Virgo observations were part of the ISO Central Program, while the Coma galaxies were observed in the open time. The  $32 \times 32$  pixel long-wavelength camera was used to make a raster map covering largely the galaxy image, with a shift (then overlap) of 16 pixels between successive positions. The pixel size was  $6'' \times 6''$ . For Virgo, the elementary integration time was 2 seconds, and 16–20 integrations were used per position. For the fainter Coma galaxies, the integration time was 5 seconds, with 10 integrations per position. A more complete description of the observations and reductions will be presented in future papers. The images were calibrated as indicated in the ISOCAM manual. The total fluxes were determined using the IMCNTS routine in IRAF/Xray after subtraction of the sky background. The fluxes are believed to be accurate to within 30%, mainly due to calibration errors. However the accuracy in the relative fluxes obtained for different objects is expected to be considerably better.

### 3. Mid-IR emission of galaxies and relation to star formation

All the fluxes in the various wavelength bands are normalized to the flux in the K' band ( $2.1 \mu\text{m}$ ; Boselli et al. 1997) for the Virgo galaxies. For the Coma galaxies, the near-IR measurements are in the H band ( $1.65 \mu\text{m}$ ; Gavazzi et al. 1996b, 1996c). Since  $H-K' = 0.26$  on average for spiral galaxies with a small dispersion (Gavazzi et al. 1996a) the fluxes for the Coma galaxies have been re-normalized to the K' band. The fluxes in both K' and H are proportional to the total stellar mass of the galaxies, which is well traced by the near-IR emission (Gavazzi et al. 1996a). All fluxes are expressed in jansky units.

In what follows, we will correct the mid-IR fluxes for the stellar contribution. This contribution is estimated from observations of 8 elliptical and S0 galaxies which fell serendipitously in the field. All these galaxies have obviously very little interstellar matter and star formation and can be used as templates. From the average of the flux ratios for these galaxies we adopt the following flux ratios for an old stellar population:

$$\begin{aligned} \log[F(6.75)/K'] &= -0.8, \quad \log[F(15)/K'] = -1.2, \\ \log[F(6.75)/F(15)] &= 0.4 \end{aligned}$$

These flux ratios are in particular those of the Virgo galaxy NGC 4649 for which we detected no  $H\alpha$  emission, and whose spectral energy distribution suggests that its 6.75 and  $15 \mu\text{m}$  emission is dominated by the Rayleigh-Jeans tail of the old stellar component (Boselli et al., in preparation).

We first present in Fig. 1 the infrared two-color diagram for galaxies with  $\log[F(6.75)/K']_{\text{uncorrected}} > -0.55$  in order to minimize errors due to the somewhat uncertain correction for the stellar contribution. Only detected galaxies are included. Far-IR fluxes at 60 and  $100 \mu\text{m}$  are taken from IRAS (Thuan

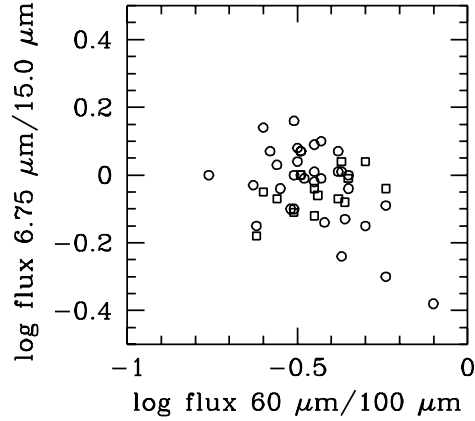


**Fig. 1.** The relation between the mid-IR flux ratio  $6.75 \mu\text{m}/15 \mu\text{m}$ , corrected for stellar contribution, and the far-IR flux ratio  $60 \mu\text{m}/100 \mu\text{m}$ . Virgo galaxies are marked with circles, Coma objects with squares.

& Sauvage 1992, Bica & Giovanelli 1987 and references therein). It appears that galaxies with a higher  $60/100 \mu\text{m}$  ratio have a lower  $6.75/15 \mu\text{m}$  ratio. Statistical correlation tests (Cox, Kendall) show that the effect is statistically significant. Although systematic errors can arise as a function of source brightness due to imperfect correction for the remanence of the detector, they are not large enough to produce the observed effect: in particular, the fainter, more distant Coma galaxies exhibit the same behaviour as the Virgo galaxies.

Figure 2 shows the normalized mid- and far-IR fluxes (the latter from IRAS) as a function of the normalized far-UV ( $2000 \text{ \AA}$ ) flux (Deharveng et al. 1995 for Virgo; Donas et al. 1990, 1995 for Coma) for all galaxies with available data. For comparison, the relation between the 60 and the  $100 \mu\text{m}$  flux from IRAS and the far-UV flux is displayed on Fig. 2c and 2d respectively. The UV flux is an excellent (although somewhat qualitative due to internal extinction in the galaxies) tracer of the rate of star formation (Boselli 1994). At low UV fluxes until  $\log[F(\text{UV})/K'] = -1.5$ , there is a proportionality between all the IR fluxes and the UV flux, suggesting that dust emission is proportional to the star formation rate (SFR). At higher UV fluxes, the mid-IR fluxes saturate and might even decrease. The different behaviour of the MIR and FIR emission of the observed galaxies cannot be explained by the extinction of the UV fluxes, which has been estimated to be  $\sim 0.9\text{--}0.2$  mag (Buat & Xu 1996).

In our Galaxy, the interstellar emission at  $6.75 \mu\text{m}$  is known from previous ISO observations to be due to the UIBs and associated continuum as long as the interstellar radiation density is not extremely high (Cesarsky et al. 1996b). At  $15 \mu\text{m}$ , while there is also a contribution of the UIBs and associated continuum, very small grains (Désert et al. 1990) also contribute at radiation densities  $\geq 10^4$  times the radiation density near the Sun. At  $60 \mu\text{m}$ , both very small grains and larger grains in thermal equilibrium contribute while the bigger grains dominate at  $100 \mu\text{m}$  (Désert et al. 1990). We recall that the carriers of the UIBs and associated continuum (that we will designate further

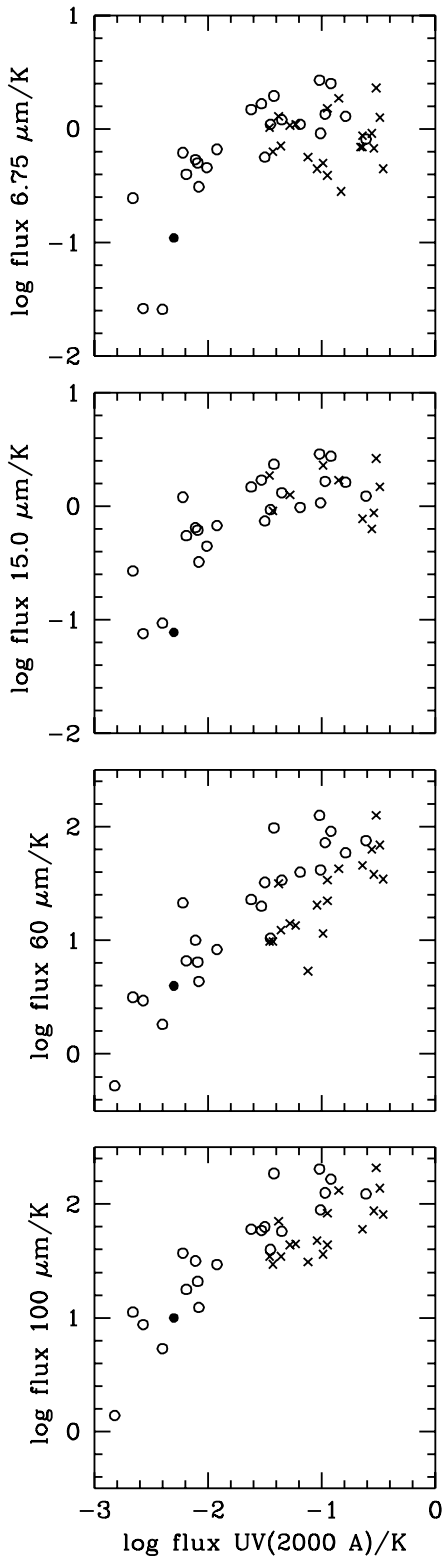


**Fig. 2.** The relation between the UV 2000 Å flux and a) the flux at 6.75  $\mu\text{m}$  corrected for the stellar contribution, b) the flux at 15  $\mu\text{m}$  corrected for the stellar contribution, c) the flux at 60  $\mu\text{m}$  d) the flux at 100  $\mu\text{m}$ . All fluxes are normalized to the K' flux. The UV fluxes are not corrected for internal extinction. The filled circle is for an early-type galaxy, the open circles for late-type galaxies with  $M_K$  brighter than -21.6 and the crosses for fainter late-type galaxies.

as Polycyclic Aromatic Hydrocarbons or PAHs although their exact nature is not known) are heated in non-equilibrium by absorption of single photons and reach temporarily very high temperatures, at which most of the emission occurs. Their emitted spectrum is thus very little dependent on the spectral energy distribution of the incoming photons although there exist some spectral variations (see Cesarsky et al. 1996a and Abergel et al. 1996). The big grains which emit at 60  $\mu\text{m}$  and dominate at 100  $\mu\text{m}$  are in thermal equilibrium, and their temperature and emitted spectrum depend directly on the interstellar radiation density. The very small grains are smaller 3-dimensional particles in an intermediate situation and their temperature and emitted spectrum depend less on the radiation field than for the big grains.

The global interstellar emission of a galaxy results from the superimposition of the emission of regions with a large range of radiation fields. In regions of small radiation field, the emission in the mid-IR is entirely due to PAHs and is simply proportional to the product of the radiation field density by the column density of dust. In our Galaxy, the corresponding flux ratio (in Jy units)  $F(6.75)/F(15)$  is between 1.0 and 1.8, (Cesarsky et al. 1996a and Abergel et al. 1996). The observed  $F(6.75)/F(15)$  ratio (corrected for stellar contribution) for galaxies with a low SFR is compatible with these values (Fig. 1), suggesting that their mid-IR emission is mainly due to PAHs. In our Galaxy, the  $F(6.75)/F(15)$  ratio seems to increase at higher UV radiation fluxes. This is a trend opposite to that of Fig. 1, showing that the latter must be due to another cause.

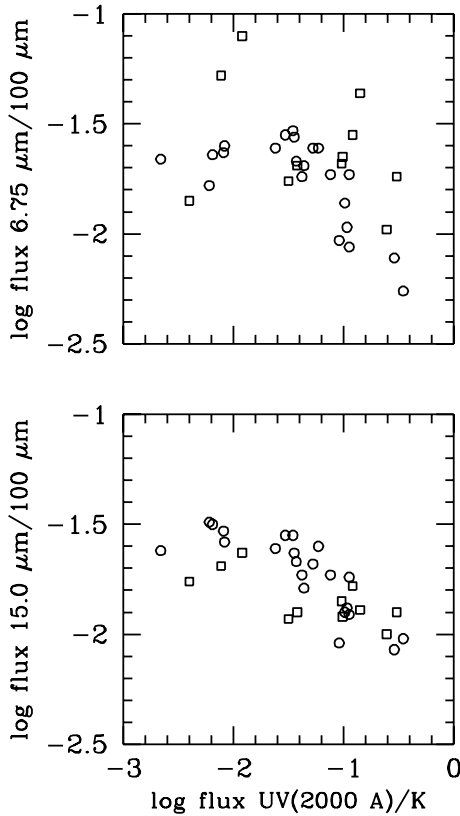
When the rate of star formation increases, the mean radiation field is stronger. Also, the fraction of interstellar matter submitted to high radiation fields near regions of star formation increases. As the large dust grains and also the very small, 3-dimensional grains are warmer, the global 60/100  $\mu\text{m}$  intensity ratio increases. The 6.75/15  $\mu\text{m}$  flux ratio decreases because the contribution of very small grains to the flux at 15  $\mu\text{m}$  becomes important. This explains the negative correlation between the 6.75/15  $\mu\text{m}$  and the 60/100  $\mu\text{m}$  flux ratios displayed in Fig. 1. The origin of this correlation is similar to that between the 12/25  $\mu\text{m}$  and the 60/100  $\mu\text{m}$  ratios which has been extensively studied, initially by Helou (1986).

Figure 2 shows a saturation or even decrease in the normalized mid-IR fluxes at high star formation rates. This can be due *a priori* to two different factors:

i) PAHs have different properties in high-SFR, low-metallicity galaxies.

ii) the abundance of all grains including PAHs is lower because the abundances of heavy elements are statistically smaller in galaxies with a high SFR, which are mainly low-luminosity spirals and irregulars. This is well-known for the big grains which are responsible for the extinction in the visible (see e.g. Bouchet et al. 1985).

Figure 3 sheds light on the problem. Figure 3a shows the ratio  $F(6.75)/F(100)$  as a function of  $F(\text{UV})/K'$ , and Fig. 3b the same for the  $F(15)/F(100)$  ratio. It is clear that both ratios decrease at higher SFRs (or lower metallicities), suggesting that metallicity is not the dominant factor of the saturation of



**Fig. 3.** The relation between the UV 2000 Å flux normalised to the K' flux and a) the flux ratio 6.75/100  $\mu\text{m}$  and b) the flux ratio 15/100  $\mu\text{m}$  for galaxies with  $\log[F(6.75)/K']_{\text{uncorrected}} > -0.55$ ; both 6.75 and 15  $\mu\text{m}$  fluxes are corrected for the stellar contribution. Open circles are for Virgo galaxies, open squares for Coma objects.

the mid-IR fluxes, since it would affect in a similar way the different types of grains then the fluxes in the different bands. The observed turn-over in Fig. 2 is probably more related to a change in the properties of the PAHs than to a metallicity effect.

#### 4. Conclusion

The present analysis is in qualitative agreement with the predictions that can be made from detailed mid-IR studies of interstellar matter in Galaxy. In spiral and irregular galaxies, the integrated emission around 7  $\mu\text{m}$  is almost entirely due to the carriers of the UIBs (“PAHs”). The integrated emission at 15  $\mu\text{m}$  is also dominated by PAHs in late-type galaxies with a low SFR, but the very small grains (Désert et al. 1990) give a important contribution in high SFR, lower-mass, late-type spirals and irregulars. The emission at both 6.75 and 15  $\mu\text{m}$  is not proportional to the star formation rate for the latter galaxies, probably due to a strongly decreasing amount of both PAHs and perhaps also of very small grains: we suggest that this decrease corresponds to different properties of PAHs in high-SFR, low-metallicity galaxies.

The mid-IR emission of a few early-type galaxies observed serendipitously in our sample is dominated by stars.

#### References

- Abergel A., Bernard J.-P., Boulanger F. et al. 1996, *A&A* 315, L329  
 Bica M. & Giovanelli R., 1987, *ApJ* 321, 645  
 Binggeli B., Sandage A., Tammann G., 1985, *AJ* 90, 1681  
 Boselli A. 1994, *A&A* 292, 1  
 Boselli A., Tuffs R., Gavazzi G., Hippelein H., Pierini D., 1997, *A&AS*, 121, 507  
 Bouchet P., Lequeux J., Maurice E., Prévot L., Prévot-Burnichon M.-L. 1985, *A&A* 149, 330  
 Buat V. & Xu C., 1996, *A&A*, 306, 61  
 Cesarsky D., Lequeux J., Abergel A. et al. 1996a, *A&A* 315, L305  
 Cesarsky D., Lequeux J., Abergel A. et al. 1996b, *A&A* 315, L309  
 Deharveng J.M., Sasseen T., Buat V., Bowyer S., Lampton M., Wu X., 1994, *A&A* 289, 715  
 Désert F.-X., Boulanger F., Puget J.-L. 1990, *A&A* 237, 215  
 Donas J., Buat V., Milliard B., Laget M., 1990, *A&A* 235, 60  
 Donas J., Milliard B., Laget M., 1995, *A&A* 303, 661  
 Gavazzi G., Pierini D., Boselli A., 1996a, *A&A* 312, 397  
 Gavazzi G., Pierini D., Boselli A., Tuffs R., 1996b, *A&AS* 120, 489  
 Gavazzi G., Pierini D., Baffa C., Lisi F., Hunt L., Randone I., Boselli A., 1996c, *A&AS* 120, 521  
 Helou G. 1986, *ApJ* 311, L33  
 Thuan T. & Sauvage M., 1992, *A&AS* 92, 749